Semiconductor-To-Metal Transition in V_2O_3*

JULIUS FEINLEIB†
Division of Engineering and Applied Physics, Harvard University, Cambridge, Massachusetts
and
Lincoln Laboratory, Massachusetts Institute of Technology,‡ Lexington, Massachusetts
AND
WILLIAM PAUL
Division of Engineering and Applied Physics, Harvard University, Cambridge, Massachusetts

(Received 20 September 1966)

This paper reports measurements of the shift with hydrostatic pressure and uniaxial stress of the temperature for a metal-to-semiconductor transition in V_2O_3; of the change with pressure and uniaxial stress of the resistivity in the metallic phase and the activation energy for condution in the semiconducting phase; and of the optical transmissivity in both phases. The results are first interpreted on the basis of a model involving a crystalline distortion to lower symmetry in the semiconducting phase, and the behavior of transition temperature and conduction under applied stress is shown to fit this microscopic model satisfactorily. The changes in transition temperature and energy gap with stress are also analyzed, starting from the statistical model of an energy gap which is linearly dependent on the number of activated carriers; the data are found to fit this model very well.

I. INTRODUCTION

FROM the several reviews of the properties of the transition-metal oxides,[1] it is apparent that the one-electron band theory is inadequate to explain transport in all of these materials. Notably it has been found that the magnetic oxides of the NiO class are insulators despite the apparent occurrence of partially filled $3d$ bands. Some oxides of vanadium and titanium exhibit properties characteristic of semiconductors at some temperatures and properties characteristic of poor metals at others. For example, V_2O_3 shows a practically discontinuous change of resistivity from about $10^4\ \Omega$ cm to about $10^{-3}\ \Omega$ cm near 150°K.

There have been several proposals, some involving the properties of localized electrons[2] and some band electrons,[3] to explain the semiconducting behavior in this and similar compounds, and also several proposals to explain the sharp semiconductor-to-metal transition.[4]

The initial localization at particular lattice sites may be caused by either electron-electron[5] or electron-phonon[6] interaction. Whichever is the cause, the conductivity will then follow an exponential dependence on temperature with an activation energy, as in the usual diffusion theory. The activation energy q may consist of two parts: The first is related to the production of the localizable carriers and may be zero; the second to the carrier transfer between sites. Although the activation energy is precisely defined from the conductivity according to $\sigma=\sigma_0 \exp(-q/kT)$, its relation to the electronic energy spectrum is undefined because the physical nature of the activation and "hopping" is not closely examined. Also, the optical absorption, possible in principle as a carrier activation or as a charge transfer, is not simply related to the electronic energy spectrum.

In the one-band-theory approach,[3] otherwise half-filled bands are split into a full valence and an empty conduction band by an antiferromagnetic exchange interaction. The conductivity will again show a carrier activation energy, which will be a direct measure of the exchange energy. The optical absorption will be forbidden since the bands involved have the same symmetry but breakdown of the rule will give an absorption at an energy equal to that for the carrier activation. A similar explanation of the existence of a filled valence and an empty conduction band involves lattice distortions, described in the paper by Adler and Brooks,[7] which we refer to as I.

Both approaches have been applied to explain a transition from semiconductor to metal as a function

* This work was supported in part by the U. S. Office of Naval Research, and by the Division of Engineering and Applied Physics, Harvard University.

† Present address: Lincoln Laboratory, Massachusetts Institute of Technology, Lexington, Massachusetts.

‡ Operated with support from the U. S. Air Force.

[1] See, for example, J. B. Goodenough, *Magnetism and the Chemical Bond* (Interscience Publishers, New York, 1963); or F. J. Morin, *Semiconductors*, edited by N. Hannay (Reinhold Publishing Corporation, New York, 1959); *Transition Metal Compounds*, edited by E. Schatz (Gordon and Breach Science Publishers, New York, 1964).

[2] See, for example, N. F. Mott, Phil. Mag. **6**, 287 (1961); R. R. Heikes, and W. D. Johnston, J. Chem. Phys. **26**, 582 (1957); J. H. DeBoer, and E. J. W. Verwey, Proc. Phys. Soc. (London) **A49**, 59 (1937); J. Yamashita and T. Kurosawa, J. Phys. Soc. Japan **15**, 802 (1960); **15**, 1211 (1960).

[3] See, for example, J. C. Slater, Phys. Rev. **82**, 538 (1951); F. J. Morin, Phys. Rev. Letters **3**, 34 (1959).

[4] See Mott, Ref. 2; W. Kohn, Phys. Rev. **133**, A171 (1964); J. Hubbard, Proc. Roy. Soc. (London) **A276**, 238 (1963); **A281**, 401 (1964); J. B. Goodenough, Phys. Rev. **120**, 67 (1960); J. Phys. Chem. Solids **6**, 287 (1958); Ref. 3.

[5] See Mott (Ref. 2), and Kohn and Hubbard (Ref. 4). Also, P. W. Anderson, in *Solid State Physics*, edited by F. Seitz and D. Turnbull (Academic Press Inc., New York, 1963).

[6] T. Holstein, Ann. Phys. (N. Y.) **8**, 325, 343 (1959); for several papers on the "small" polaron, see *Polarons and Excitons*, edited by J. Kuper, and G. Whitfield (Oliver and Boyd Publishers, London, 1963).

[7] D. Adler and H. Brooks, preceding paper, Phys. Rev. **155**, 826 (1967).

of volume or of temperature. In the band-theory method, the solid is a semiconductor below the Néel temperature, and a metal above it, or alternatively, a semiconductor or a metal according to whether there exists a lattice distortion or not. The transition from semiconductor to metal as a function of temperature may be sharp, as has been most graphically argued in I.

The second approach views the transition as one from conduction by "hopping" electrons to conduction by "flowing" or band electrons. In 1949, Mott[8] argued that, quite generally, any periodic array of atoms, and particularly one whose atoms had an odd number of electrons in their outermost shells, would behave like a perfect insulator at sufficiently large interatomic distances. On the other hand, the very existence of metals required that odd-electron atoms form metals at the normal lattice constants. Mott argued further that the transition of a function of interatomic separation would be very sharp and would occur when the electron-hole attraction was shielded by a high density of carriers. That the material be an insulator at large interatomic distances is intuitive from our knowledge of atoms and the simplest molecules, and depends obviously on electron correlation effects. Quantitative many-electron treatments by Kohn[4] and by Hubbard[4] more recently have established this part of the solution on a firm basis, and have shown that the low conductivity is not just due to a very greatly increased value of the effective mass. However, the treatment of the region of transition from semiconductor to metal, where electron correlation effects are still large, but also the tendency for electrons to spread out into bands is also large, is a good deal harder and has not been satisfactorily completed. The present position seems to be that the theory shows the transition to be sharp or gradual depending on the approximations that have been made in order to reduce the problem to one that is analytically manageable.

Since the separation of the ions appears as an important parameter in these theories, we have studied the effects of hydrostatic and uniaxial stresses on transport in both the semiconducting and metallic phases of V_2O_3 and on the transiton temperature between the two. We have thereby been enabled to establish to what extent these models apply to this specific solid. In particular, we have examined the possible applicability to this situation of the statistical model presented in I.

In order to set the investigation on V_2O_3 in perspective, we shall first describe the properties of this compound other than those reported in the main body of the paper. At room temperature, V_2O_3 has a corundum structure[9] with rhombohedral symmetry: There is a unique c axis perpendicular to the basal plane which contains three identical crystal axes. Near 150°K, a phase transition occurs to monoclinic.[9] The symmetry change may be thought of as occurring by a pairing

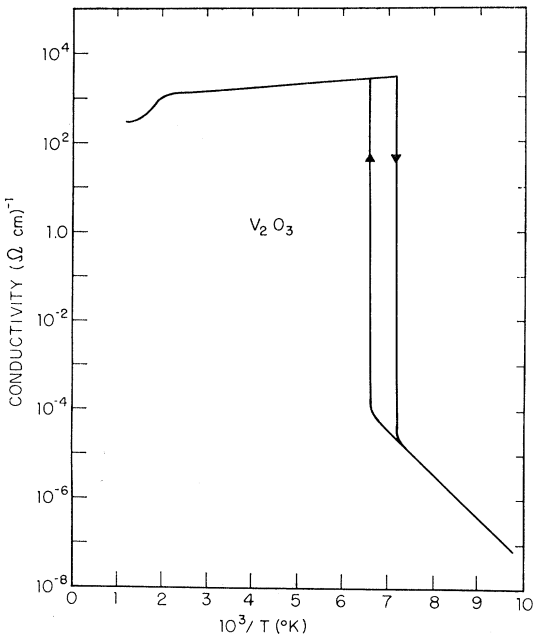

FIG. 1. Conductivity versus temperature for a single-crystal sample of V_2O_3.

distortion of the vanadium ions along one of the three basal plane axes, and a simultaneous tilting of the c axis. The volume increases by 3.5% in the transition to the low-temperature phase.[10] The crystal structure is illustrated in Fig. 6.

The transition is accompanied by a change in magnetic susceptibility,[11] but no magnetic ordering transition has been definitely confirmed by neutron diffraction.[12] Nuclear-resonance data at the transition appear to favor an antiferromagnetic ordering,[13] although the local magnetic moment is less than 0.5 Bohr magnetons.[12] Recent Mössbauer measurements show that there is a static hyperfine field at low temperatures which disappears at the transition. This is consistent with an antiferromagnetic ordering, but the temperature dependence of the internal field shows that it is probably the crystal structure change which is primarily responsible for the transition. Other changes at the transition from semiconductor to metal are observed in the specific heat[14] and thermoelectric power.[15] The most striking change, in the resistivity, is illustrated in Fig. 1.

[8] N. F. Mott, Proc. Phys. Soc. (London) **A62**, 416 (1949).
[9] E. P. Warekois, J. Appl. Phys. Suppl. **31**, 346 (1960).
[10] S. Minomura and H. Nagasaki, J. Phys. Soc. Japan **19**, 131 (1964).
[11] M. Foex, J. Goldsztaub, R. Jaffrey, R. Lyand, R. Wey, and J. Wucher, J. Rech. Centre Natl. Rech. Sci. Lab. Bellevue (Paris) **21**, 237 (1952); P. H. Carr and S. Foner, J. Appl. Phys. Suppl. **31**, 344 (1960).
[12] S. C. Abrahams, Phys. Rev. **130**, 2230 (1963); A. Paoletti and S. J. Pickart, J. Chem. Phys. **32**, 308 (1960).
[13] E. D. Jones, Phys. Rev. **137**, A978 (1965).
[14] C. T. Anderson, J. Am. Chem. Soc. **58**, 564 (1936).
[15] A. J. MacMillan, Laboratory for Insulation Research, MIT Technical Report No. 172, 1962 (unpublished).

II. TRANSPORT MEASUREMENTS

A. Metallic Region

A full description of the history and processing of the single-crystal samples used, of the pressure and stress apparatus, and of the other techniques involved, is given in a technical report from our laboratory.[16] The general features of the temperature dependence of the resistivity have previously been reported for ceramic materials, and for single crystals. The single crystals used in this investigation appear to be at least as pure and stoichiometric as any hitherto used, and several new features of the resistivity curve have been added.

Figure 2 shows the resistivity, normalized to the 0°C value, for the two principal crystallographic directions in the temperature range from 350°K down to the metal-semiconductor transition near 150°K. The absolute values of resistivity are

$$\rho_{11}(0°\text{C}) \text{ (basal plane)} = 6.3\times10^{-4}\,\Omega\text{ cm},$$
$$\rho_{33}(0°\text{C}) \text{ (c axis)} = 5.6\times10^{-4}\,\Omega\text{ cm}. \quad (1)$$

The error in absolute value is $\pm10\%$ because of the difficulty in obtaining accurate length measurements at the soldered contacts. The agreement among several samples was within 5%. The anisotropy is seen to be small and the anisotropy ratio, defined as $\rho_{33}(T)/\rho_{11}(T)$, is 0.9 at 0°C. In this temperature range the resistivity is seen to be a linear function of temperature with a positive coefficient and is calculated to be

$$\rho(T)/\rho(0°\text{C}) = 0.36+2.3\times10^{-3}T(°\text{K}). \quad (2)$$

The characteristic metallic resistivity shows anomalous behavior at higher temperatures, as seen in Fig. 3. Both the c axis and basal plane resistivities show a rapid increase with temperature in the region near 525°K, but remain monotonically increasing up to the highest temperatures. This result is in sharp contrast with that

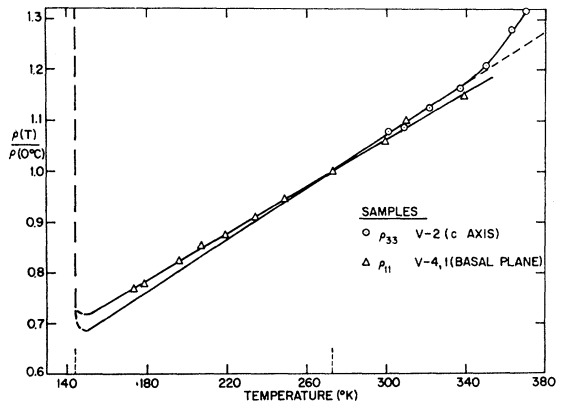

FIG. 2. Resistivity versus temperature for two directions in single crystal V_2O_3.

[16] J. Feinleib, Gordon McKay Laboratory, Harvard University, Technical Report No. HP-11, 1963 (unpublished).

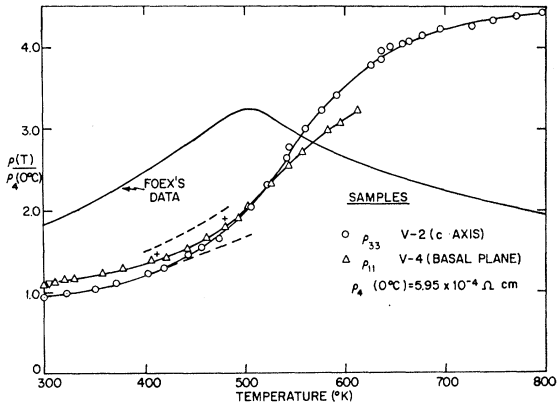

FIG. 3. High temperature resistivity of V_2O_3, showing anomalous behavior near 525°K. Data by Foex (Ref. 17) on sintered bars are also included.

reported by Foex.[17] In his measurements on sintered bars of V_2O_3, there is a similar rise in resistivity with temperature until a maximum is reached near 525°K. With further increase in temperature his data show a decrease in resistivity which is linear on a plot of $\log\rho$ versus $1/T$ and yield an activation energy for conduction of 0.04 eV. The absolute resistivities of our single-crystal samples are about $10^{-3}\,\Omega$ cm in this range compared to about $2\times10^{-2}\,\Omega$ cm for the sintered material. We may also note that the anisotropy ratio for our crystals has increased only to a value of 1.1 at 625°K.

This high-temperature anomaly in the resistivity of V_2O_3 is found to be accompanied by an anomaly in specific heat,[11] a marked change in magnetic susceptibility,[11] and an anomalous change in expansion coefficient.[11]

The pressure effect on the room temperature resistivity for the two crystal orientations is shown in Fig. 4. The decrease of resistance with pressure is similar to that observed in several other metals.[18] It is seen that the anisotropy in resistivity is decreased by pressure, an effect observed by Bridgman[18] for metals such as Zn, Cd, and Sn. The initial pressure coefficients are

$$\left(-\frac{1}{\rho_{33}}\frac{\partial\rho_{33}}{\partial P}\right) = (7.6\pm0.2)\times10^{-6}\,\text{bar}^{-1},$$
$$\left(-\frac{1}{\rho_{11}}\frac{\partial\rho_{11}}{\partial P}\right) = (14.0\pm0.2)\times10^{-6}\,\text{bar}^{-1}. \quad (3)$$

B. Transition from Metal to Semiconductor

The temperature of the transition from metal to semiconductor in V_2O_3 has been variously reported to

[17] M. Foex (Ref. 11).

[18] For a recent review, see W. Paul, *High Pressure Physics and Chemistry*, edited by R. S. Bradley (Academic Press, Inc., London, 1963), p. 299.

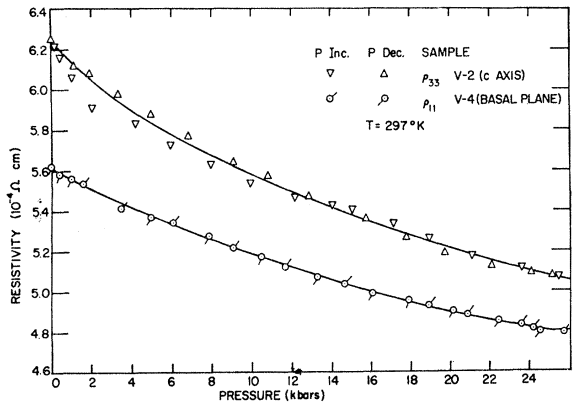

FIG. 4. Resistivity versus hydrostatic pressure for oriented samples of V_2O_3.

range from 168°K in sintered materials to 140°K in single crystals. The measurements on our crystals indicated a transition at atmospheric pressure to occur at 140±2°K. The reverse transition on heating was less well defined because the samples usually fractured, but a best estimate would be 151±3°K. The transition in the single crystal material had the following characteristics:

(1) There is a gradual change in resistivity starting at about 1°K from the transition on the metallic side, and then a very rapid change in a few hundredths of a degree.

(2) On the semiconducting side, the resistivity changes slowly over a 5°K interval before a stable, linear $\ln\rho$ versus $1/T$ behavior is obtained. From the last result, it is found that our single crystals have a change in resistivity by about two orders of magnitude greater than that reported for other materials. The low-transition temperature in our samples may be closer to the true transition point of pure material than the higher temperatures reported by others. This may seem contrary to the expected behavior, but MacMillan[15] has shown that most impurities in V_2O_3 tend to raise the transition temperature as well as to decrease the amount of resistivity change at the transition.

(3) The resistivity changes from the beginning to the end of the transition by a factor of 10^7.

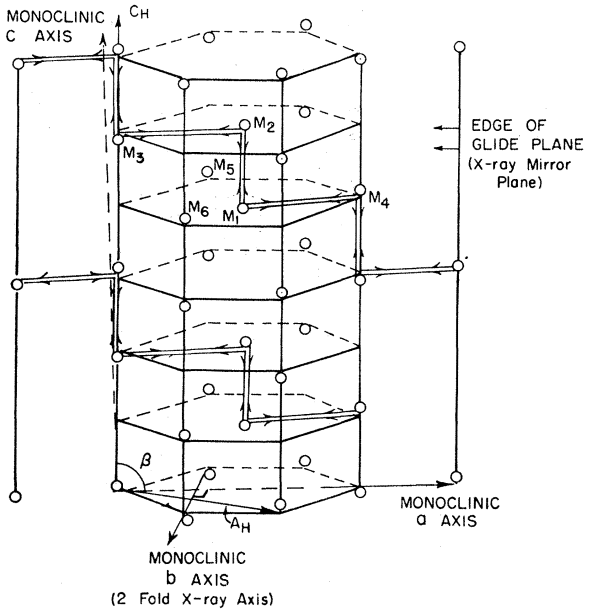

FIG. 6. Simplified structure of V_2O_3 showing only vanadium ion positions.

C. Effect of Stress on Transition Temperature

Figure 5 summarizes the results of the effect of hydrostatic pressure on the metal to insulating transition temperature. The data were taken by two techniques: holding the pressure constant and varying the temperature at a rate of about 0.5°C/h in the transition region; holding the temperature constant and varying the pressure at a rate of about 10 bar/min. The samples used were single crystals which invariably fractured after one transition. The return transition to the metallic state was more sluggish, presumably because of

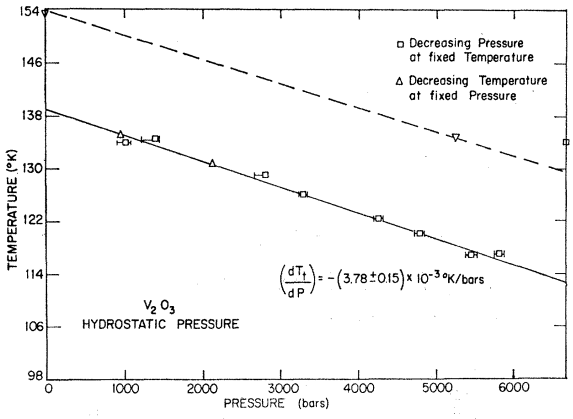

FIG. 5. Transition temperature versus hydrostatic pressure.

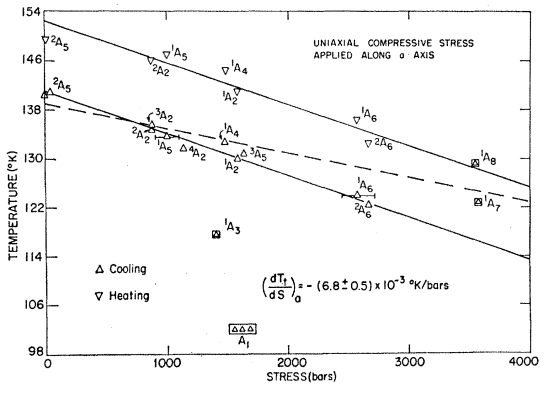

FIG. 7. Transition temperature versus uniaxial stress along the *a* axis.

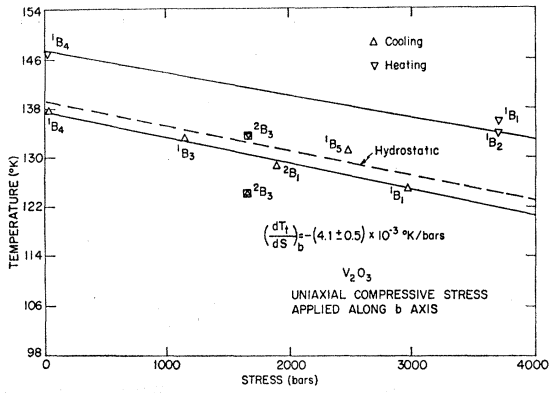

FIG. 8. Transition temperature versus uniaxial stress along the b axis.

the sample fracturing, and the data are indicated by the broken line.

The slope obtained from the curve is calculated to be

$$(dT_0/dP) = (-3.78 \pm 0.15) \times 10^{-3} \text{ °K/bar}. \quad (4)$$

This result is in agreement with that obtained by Austin[19] by a quasihydrostatic technique.

Measurements were made of the effect of uniaxial stress on the transition temperature for the three principal sample orientations. The sample orientation refers to the crystallographic axis which was parallel to the applied uniaxial compressive stress. These axes are labeled according to the monoclinic structure of the semiconducting phase. Figure 6 shows the simplified structure of V_2O_3 with only the metal ions indicated and shows the relation between the monoclinic axes and the axes of the trigonal metallic phase (referred to the hexagonal system). The results are shown in Figs. 7, 8, and 9.

Most of the data points recorded are for cooling transitions, i.e., from metal to insulator, since this is the first transition undergone by each sample. For those samples in which several transitions were obtainable, the different data points for the sample are indicated by the symbol near the points: The subscript is the number of the sample, and the superscript indicates the order in which the transitions occurred. Generally, it was found that the application of uniaxial compression to the a-axis samples allowed these samples to pass through several transitions without fracturing. A few b-axis samples behaved in this manner, but no c-axis samples survived more than one transition even with stress applied. A square surrounds the points which are deemed unreliable because the sample was severely fractured upon removal from the apparatus. While the heating transition from semiconductor to metal was less well defined, all the data obtained indicated that the hysteresis in the transition remained constant, independent of stress, and that the heating and cooling curves were separated by 10–12°C. The slopes of the two curves are therefore shown parallel. The dashed curve in each figure is the hydrostatic pressure data.

From the figures above, the stress coefficients for each orientation are calculated:

$$(dT_0/dS)_a = -(6.8 \pm 0.5) \times 10^{-3} \text{ °K/bar}, \quad (5)$$

$$(dT_0/dS)_b = -(4.1 \pm 0.5) \times 10^{-3} \text{ °K/bar}, \quad (6)$$

$$(dT_0/dS)_c = -(0.5 \pm 0.5) \times 10^{-3} \text{ °K/bar}. \quad (7)$$

To make these coefficients directly comparable to the hydrostatic coefficient, the sign of the stress is chosen to be positive for a uniaxial compression. The most striking result of these experiments is the large difference between the c-axis coefficients and the others.

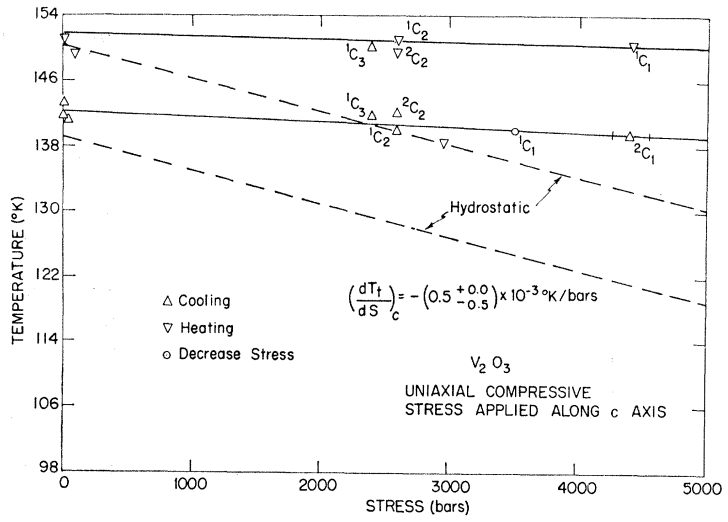

FIG. 9. Transition temperature versus uniaxial stress along the c axis.

[19] I. G. Austin, Phil. Mag. 7, 961 (1962).

D. Semiconducting Region

Accurate measurements of the transport behavior in the semiconducting region were difficult to obtain because the single crystals fractured when cooled through the transition. When it was found that the application of uniaxial stress could preserve the crystal, several measurements were made of the effect of uniaxial stress on the resistivity. The effect of hydrostatic pressure was also measured by an arrangement in which the sample in the pressure vessel was stressed uniaxially by the force of a small spring. In the two terminal measuring technique, the unavoidable effects of contact resistance reduce the accuracy of the absolute values of resistivity, but several measurements in different crystals gave fairly consistent results.

Figure 10 shows two curves of resistivity versus temperature from which the activation energy for conduction is calculated. The data for sample C_3 were taken with a constant stress of 2550 bar applied along the c axis. This sample showed some longitudinal cracks. The data for sample B_5 were taken with a uniaxial stress of 2480 bar applied along the b axis and remained intact. The resistivity is measured parallel to the stress axis. The activation energy q is calculated from the slope of the curve and is defined by the relation

$$\rho(T)=A\rho(T_0)\exp(q/kT), \tag{8}$$

where $\rho(T)$ is the resistivity at temperature T and A is a constant. The results obtained are

$$q_c=0.12\text{ eV},\quad \rho_c(132^\circ\text{K})=0.5\times10^4\,\Omega\text{ cm}, \tag{9}$$
$$q_b=0.18\text{ eV},\quad \rho_b(132^\circ\text{K})=1.3\times10^4\,\Omega\text{ cm}.$$

The constant applied stress has a very different effect on the transition temperatures of the two samples and this could also account for the difference in the resistivity and activation energy, although there are insufficient data to bear this out.

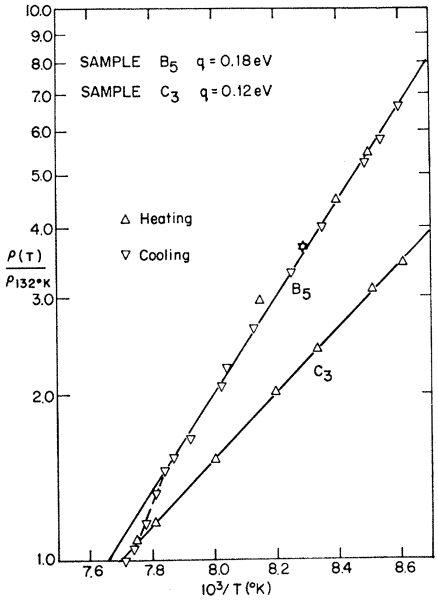

FIG. 10. Resistivity versus temperature for the semiconducting phase.

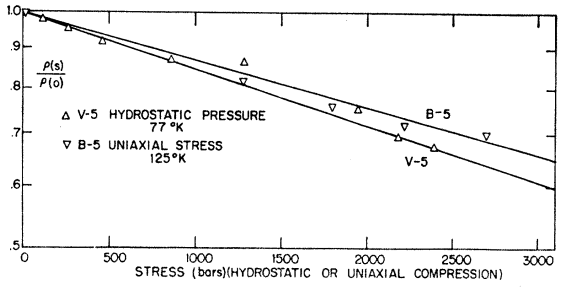

FIG. 11. Resistivity versus hydrostatic pressure and uniaxial stress for the semiconducting phase.

Figure 11 shows the results of several attempts to measure the effect of uniaxial stress and hydrostatic pressure on the resistivity of the single crystals in the semiconducting phase. There is a large scatter in the data, but a reasonably accurate hydrostatic pressure coefficient and stress coefficient for the b axis were obtained. These coefficients α are defined by the relation:

$$\rho(S,T)=A\rho(0,T_0)\exp\left(\frac{q+\alpha S}{kT}\right), \tag{10}$$

where S is the stress or hydrostatic pressure. The coefficients obtained from these data are

$$\alpha(\text{uniaxial})_b=-1.5\times10^{-6}\text{ eV/bar}, \tag{11}$$

$$\alpha(\text{hydrostatic})=-1.1\times10^{-6}\text{ eV/bar}. \tag{12}$$

A similar measurement has been made by Austin[19] using a quasihydrostatic apparatus and the less sensitive technique of holding pressure constant and varying the temperature. His coefficient is almost a factor of 5 greater and is given as approximately -5×10^{-6} eV/bar.

III. OPTICAL MEASUREMENTS

In these measurements, a single-crystal slice was cut to $\frac{1}{2}$ cm^2 cross section and then polished to a thickness of 25 μ. The crystal was kept from fracturing at the low temperature by applying a uniaxial stress through a spring while the sample was clamped between two $\frac{1}{4}$-in.-thick polished KBr plates. The holder then fitted in the cold finger of an optical nitrogen Dewar. The holder was movable in the Dewar so that in one position the light path went through the KBr plates and the sample, while in the other position, the light passed only through the KBr plates. With this arrangement, the relative optical transmission through the sample could be monitored while the sample was slowly cooled.

A Perkin-Elmer spectrometer with KBr and LiF prisms was used with a globar source and thermo-

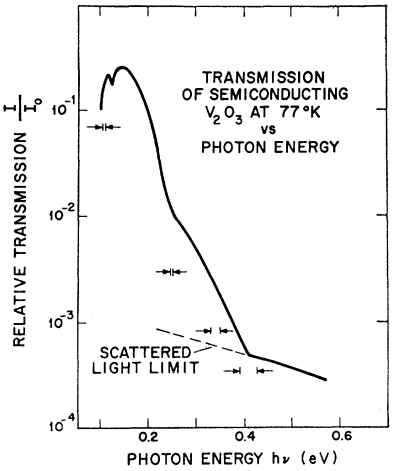

FIG. 12. Relative transmission versus photon energy for a sample 25 μ thick, at 77°K.

couple detector. With KBr windows in the Dewar and spectrometer, the system was usable to a wavelength of 20 μ.

At room temperature, in the metallic phase, no transmission was observed in the range from 20 to 0.2 μ. The sensitivity was limited by the large amount of light scattered around the sample through the KBr plates. The scattered light intensity was about 0.1% of the light incident on the sample.

As the sample was cooled, no transmission was obtained until the temperature was lower than the transition temperature. Figure 12 shows the results of the transmission measurement at 77°K. Because of the large amount of scattered light, shown as the dashed curve, it was difficult to calculate the absolute absorption coefficient α, as given by $I/I_0=-e^{-\alpha x}$, where x is 25 μ for our sample. A rough estimate is that α extends from $\sim$1000 at the transmission maximum to $\sim$3000 where the scattered light masks the transmission. No correction was made for the reflectivity since it has not been measured for the semiconducting material.

As seen in Fig. 12, the absorption edge is not sharp, but extends over several tenths of an electron volt. The calculated resolution of the instrument over the measured range is indicated on the figure. It is seen that this could not account for the large spread in energy. From the data on this one sample, it is useless to speculate on the cause of the spreadout edge. However, from the band structure contemplated for this material, it is not surprising that the edge should be different from the wide band semiconductors. We have taken the energy gap to be about 0.1 eV from this measurement because the absorption coefficient is fairly large even at this energy. Free-carrier and impurity effects could account for the high absorption coefficient at lower energies. The fine structure at low energies was reproducible for this sample, but no further measurements on other samples have been made for comparison.

IV. DISCUSSION

The transport behavior of V_2O_3 can be separated into three distinct temperature regions: the semiconducting range below 140°K, the metallic range between 140 and 525°K, and the high-temperature metallic range. The metallic behavior is most easily understood in terms of a narrow conduction band, presumably formed from the d electron orbitals of the vanadium ions; and we can obtain some quantitative characteristics of this band from the data presented here. The semiconducting phase and the transition to a metal are less well understood. It is possible that the lack of conduction comes about from the trapping of the conduction electrons on cation sites, or in cation pair bonds, whereas a band model would suggest that an energy gap forms between a filled and an empty band of Bloch electron states. In the latter case, the activation energy for conduction refers only to the production of free carriers, whereas in the former there is also an activation energy for the mobility.

A. The Metallic Region

A qualitative idea of the conduction in the metallic phase is afforded by an examination of the driving force for the transition from semiconductor to metal. The discontinuity in volume and entropy at the transition are associated with a latent heat L, given by

$$L=T_0\Delta S,$$

where ΔS, the total change in entropy between the two phases, is composed of electronic terms, lattice terms, and spin-ordering terms.

$$\Delta S=\Delta S_{\text{electronic}}+\Delta S_{\text{lattice}}+\Delta S_{\text{spin}}.$$

The latent heat may be calculated from the Clausius-Clapeyron relation for a first-order transition,

$$(dP/dT)_{T_0}=L/T_0\Delta V.$$

That the transition is first order has been established by the measurements of lattice constant change at the transition of Minomura and Nagasaki.[10] Their volume change, and our pressure coefficient and transition temperature combine to give

$$L=1020 \text{ cal/mole}=0.044 \text{ eV per } V_2O_3 \text{ formula unit}.$$

Indirect arguments suggest that magnetic effects are not the main cause. From neutron-diffraction measurements Abrahams has put an upper limit of 0.2 Bohr magnetons on the local moment near T_0. Although we cannot calculate the spin-ordering contribution ΔS_{spin} directly, we may estimate it by comparison with the work of Bean and Rodbell[20] on MnAs. In this material, a first-order magnetic transition occurs, and these workers have calculated and measured the spin ordering

[20] C. P. Bean, and D. S. Rodbell, Phys. Rev. **126**, 104 (1962).

entropy change to contribute about 234 cal/mole to the latent heat. The local moment in MnAs is larger than the upper limit given to that in V_2O_3 and therefore this contribution to the latent heat is probably the upper limit to that expected in V_2O_3. We may thus conclude that the ΔS_{spin} term and therefore the magnetic contribution to the transition in V_2O_3, is not as important as other factors.

The electronic entropy change may be more easily estimated. We may assume the electronic entropy in the semiconducting phase to be sensibly zero, because of the small number of carriers. The entropy of the carriers in the metallic phase may be estimated by assuming the simplest possible model of a spherical Fermi surface and a parabolic energy band. Then $|\Delta S_{\text{electronic}}| = z\pi^2k^2T_0/2E_F$, where E_F is the Fermi energy measured from the bottom of the band, and z is the number of conduction electrons per molecule.

If we were to ignore the contribution of $\Delta S_{\text{lattice}}$, then $L=T_0\Delta S=z\pi^2k^2T_0/2E_F$. Insertion of the values for L and T_0 leads to an E_F of 0.07 eV. The Fermi energy has been estimated from the theory of I, and is in substantial agreement with this value. A complete comparison of the theory and the experimental data is made in Ref. 21, referred to as III. This value must be corrected for lattice entropy changes, which are taken to include contributions from the changes in the phonon spectrum, changes in the lattice symmetry, and changes in the states of electrons other than conduction electrons. There are in the literature arguments for entropy changes of the order of k per molecule, of either sign.[22] If it is indeed of this order the Fermi energy will be changed by about 0.02 eV. The exact number is not important, for it does appear that the bandwidth in the metallic conduction band is very narrow, say of the order of 0.2 eV at most. We can use this value in the formula

$$E_F=(\hbar^2/2m^*)(3\pi^2N)^{2/3},$$

where N is the carrier concentration, to calculate an effective mass of $50m$, and the conductivity data quoted earlier to give a mobility and relaxation time:

$$\mu=\sigma/Ne=0.2\ \text{cm}^2/\text{V sec},$$

and

$$\tau=\mu m/e\times m^*/m=6\times10^{-15}\ \text{sec}.$$

The relaxation time is of the order found in typical metals. The mobility, however, is much lower than that in metals such as copper ($\mu\sim30$ cm^2/V sec). The carriers in V_2O_3 metal are therefore slower because of their large effective mass, and therefore have a smaller mean free path in the crystal than in typical metals. This is seen from the following calculation of carrier velocity at the Fermi surface U_F and the mean free path l:

$$U_F=(2E_F/m^*)^{1/2}=3\times10^6\ \text{cm/sec},$$
$$l=\tau U_F=2\ \text{Å}.$$

For V_2O_3, a mean free path of 2 Å is of the order of one lattice constant. In copper, the corresponding number is about 100 lattice constants. This, therefore, is the extreme narrow-band limit for the concept of band states. In fact, the uncertainty in energy of the carriers with the relaxation time given is $\sim$0.1 eV which is a large fraction of the bandwidth of 0.2 eV.

B. The Semiconducting Region

The activation energy for conduction lies between 0.12 and 0.18 eV. Our optical measurements indicate that the band gap is about 0.1 eV so that, in an intrinsic material, the activation energy for the production of carriers would account for 0.05 eV of the total. The remaining large fraction of the activation energy is presumably related to the hopping motion of localized electrons and should lead to a mobility substantially lower than in the metallic region. That hopping may occur in this substance is not surprising in view of the narrowness of the bands even in the metallic state. We speculate that the large-carrier density increase at T_0 leads to greatly increased screening of the electrons from the ions, which eliminates the mobility activation energy entirely, and converts hopping electron conduction by a few electrons to conduction by N electrons per cc moving in a narrow band.

C. The Semiconductor-to-Metal Transition

The pressure and stress coefficients of the transition temperature are given in Eqs. (4)–(7). A comparison of these numbers leads to several conclusions about the nature of the transition. First we note that hydrostatic pressure reduces the transition temperature, thus favoring the metallic phase. For a linear extrapolation, the material would be matallic to 0°K with about 40 kbar of applied pressure. Qualitatively, we may conclude that if the transition is caused by a crystal-structure distortion, as it apparently is, then external pressure prevents the distortion and tends to keep the crystal in the higher symmetry state of the metal phase. This may be illustrated by an examination of Fig. 6.

In the metallic phase vanadium ions M_4, M_5, and M_6 are equidistant from vanadium ion M_1. When the distortion occurs to the semiconducting phase, the distance between M_1 and M_4 decreases relative to M_5–M_1 and M_6–M_1. The effect of hydrostatic pressure is to compress the lattice, thus making it less necessary for the crystal to distort so as to reduce M_1–M_4, and prolonging the metallic phase to lower temperature. This interpretation is supported by the effects of uniaxial stress. The distortion occurs in the basal plane of the crystal and has

[21] D. Adler, J. Feinleib, H. Brooks, and W. Paul, following paper, Phys. Rev. **155**, 851 (1967).
[22] N. F. Mott (Ref. 2); C. P. Bean and D. S. Rodbell (Ref. 20).

little effect on the c-axis distances. We might, therefore, expect that uniaxial compression applied along the basal plane axes would depress the transition temperature more than uniaxial compression along the c axis. This is borne out by the uniaxial stress coefficients of Eqs. (5), (6), and (7). We may also note that the uniaxial stresses in the basal plane have a greater effect on the transition temperature than the hydrostatic stress, as one would expect from this argument.

The theories explaining the semiconductor-to-metal transition are concerned with intrinsic materials, and in particular the theory in I has predicted a relation between the intrinsic energy gap and transition temperature. This theory also predicted that the logarithmic derivatives of the energy gap and transition temperature with respect to an external parameter such as stress, should be equal. In practice, we have not measured the stress and pressure coefficients of the energy gap, but have measured the coefficients of the conductivity activation energies as given in Eqs. (11) and (12). However, we may argue that these coefficients are related to the change in energy gap so that

$$\frac{d(E_g^0/2)}{dX}=\frac{dq}{dX}. \tag{13}$$

The quantity q contains both the activation energy for carrier production $Eg/2$ and the activation energy for hopping E_H. Experimental evidence on NiO[16] indicates that the pressure dependence of E_H is an order of magnitude smaller than that measured for q in V_2O_3. Also, in III, a rough estimate is made of the pressure coefficient of the polaron hopping energy, starting from Holstein's relations for "small" polarons. Again it is found that the pressure coefficient is much smaller than those measured here for $q=(E_g^0/2)+E_H$.

A direct measure of the change in energy gap with pressure could be obtained from a measurement of the optical gap with pressure. Owing to the considerable difficulty in obtaining the optical transmission measurements in available samples, this was not done and we must rely on the values deduced from conductivity and given by (12) for comparison with theory.

Table I lists the logarithmic derivatives of energy gap and transition temperature for applied hydrostatic pressure and two directions of uniaxial stress. The equality as predicted by the theory in I holds remarkably well. A further comparison of results is made in III.

TABLE I. Pressure and uniaxial stress coefficients of the transition temperature and energy gap in V_2O_3.

$\frac{d\ln T_0}{dP}=-2.6\times10^{-5}$ bar^{-1}	$\frac{d\ln E_g^0}{dP}=-2.2\times10^{-5}$ bar^{-1}
$\left(\frac{d\ln T_0}{dS}\right)_b=-2.8\times10^{-5}$ bar^{-1}	$\left(\frac{d\ln E_g^0}{dS}\right)_b=-3.0\times10^{-5}$ bar^{-1}
$\left\|\left(\frac{d\ln T_0}{dS}\right)_c\right\|<0.3\times10^{-5}$ bar^{-1}	...

D. Discussion of Other Models for the Transition and for the Conduction Processes

The results obtained permit a comparison of several other models that have been proposed to explain the semiconductor-to-metal transition in V_2O_3 and the main features of the conduction process.

(1) Morin had suggested the Slater model for V_2O_3 with T_0 as the Néel temperature. The difficulties of this model are (a) the magnetic-ordering transition is in doubt, (b) even if it occurs, the associated latent heat seems to be much less than that observed, (c) the crystal distortion is not incorporated, and (d) the disappearance of long-range order does not mean there is no short-range order which for these electrons of small mean free path can cause a band splitting.

(2) Mott, on the other hand, had argued that increased shielding would force a semiconductor-to-metal transition at a critical interatomic separation. Unfortunately, the lattice constant at quite low temperature in the semiconducting phase becomes smaller than it is in the high-temperature metallic phase, so that this explanation will not serve without elaboration. From our earlier discussion, we suggest that the increased shielding comes not from an increase in the density of the crystal but from a band collapse (with associated lattice distortion). This is not what Mott described but the philosophy is similar.

(3) Goodenough emphasized the role of direct electron cation-cation interaction and of critical ionic separations. He explained the transition to the semiconducting phase as a pairing of atoms in the basal plane. It is to be noted immediately from Fig. 6 that the lattice distortion at T_0 described in our introduction includes just such an atom pairing. It is also plausible that the effect of stress applied in the basal plane will be much greater in displacing T_0 or changing E_g than stress applied along the c axis. An extension of this model explains the high-temperature anomaly as a disappearance of similar c-axis pairing. We note immediately that this envisages a large anisotropy in conductivity between 140 and 525°K, and this is not found.

Thus it appears that none of the previous models are adequate in themselves, but also elements of most of them have been incorporated into the model suggested in this report.

E. The High-Temperature Anomaly; Spin-Disorder Scattering

The behavior of the resistivity at high temperatures is illustrated in Fig. 3. We shall consider together the

increase near 525°K, and the large residual resistivity indicated by Eq. (2). Some of this large residual resistivity is probably due to the large concentration of defects inherent in crystals grown by flame-fusion techniques. Another possibility is spin-disorder scattering as has been discussed by deGennes and Friedel.[23] A simple estimate of this effect has been made in III, where it is found that the temperature-independent resistivity is

$$\rho_{So}=1.4\times10^{-4}\,\Omega\,\mathrm{cm}$$

compared with the measured value in (2) of $2.2\times10^{-4}\,\Omega\,\mathrm{cm}$.

Spin-disorder scattering may also be responsible for the anomalous change in the resistivity of the metallic phase above 525°K, as shown in III. The shape of the resistivity curve seen in Fig. 3 is very similar to the resistivity change calculated by deGennes and Friedel for a spin-disorder scattering mechanism at a magnetic-ordering transition. By extrapolating the linear region of the curve in Fig. 3 to higher temperatures, we find that the added resistivity above 525°K is

$$\rho_A=12\times10^{-4}\,\Omega\,\mathrm{cm},$$

which is in good agreement with that calculated in III. While this is not strong evidence for magnetic ordering at 525°K, it is consistent with the fact that this high-temperature anomaly has been interpreted by other workers[24] to be caused by an antiferromagnetic-to-paramagnetic transition as evidenced by their magnetic susceptibility measurements. Such a transition may be a contributing part of the band rearrangement similar to the one which occurs at the semiconductor-to-metal transition.

[23] P. G. deGennes and J. Friedel, J. Phys. Chem. Solids **4**, 71 (1958).

[24] J. Wucher, Compt. Rend. **241**, 288 (1955); S. Teranishi and K. Tarama, J. Chem. Phys. **27**, 1217 (1957).

V. CONCLUSION

In this work we have established several experimental quantities concerning the semiconductor-to-metal transition which may be considered with theories describing the transition. The optical absorption measurements place the semiconducting phase energy gap at about 0.1 eV, establishing the ratio of E_g/kT_0 to be ~8. An estimate of the Fermi energy from the pressure dependence of the transition temperature has shown that even in the metallic phase, the bands involved as the conduction and valence bands are extremely narrow (~0.2 eV) when compared to better known semiconducting materials. Thus, while the mobility of carriers in the metallic phase shows that they may be represented by band carriers of high effective mass, the carriers in the semiconducting phase may have a localized character with a hopping mobility. Further, it is argued that the stress behavior of the transition temperature is consistent with a distortion to lower symmetry in the semiconducting phase, and it is suggested that this is the dominant cause of the transition. The pressure and stress coefficients of the energy gap and transition temperature, which we have measured, show a unique relation which is predicted by the theory of I. These results as well as those for other materials are compared more fully in III.